文章编号: 1001－2060(2008)05－0473－05

跨音速轴流压气机间隙泄漏流流动特性研究

张燕峰, 楚武利, 吴艳辉
(西北工业大学 动力与能源学院, 陕西 西安 710072)

摘　要: 间隙泄漏流对轴流压气机的旋转失速造成严重影响, 通过对跨音速压气机 NASA 转子 37 进行单通道非定常及多通道非定常数值模拟, 单通道非定常计算揭示, 在近失速工况下, 叶顶存在间隙泄漏流自身非定常性, 并且比较了两个不同背压条件下的非定常模拟结果, 当出口背压较大的情况下, 间隙泄漏流非定常性很不稳定, 而当出口背压较小时, 泄漏流非定常性稳定; 多通道非定常数值模拟结果显示, 在近失速工况下, 当出口背压较大的情况下, 间隙泄漏流非定常振荡, 触发突尖型旋转失速先兆, 具体表现为叶尖前缘间隙泄漏流溢出, 而当出口背压较小的情况下, 间隙泄漏流非定常性始终较为稳定。

关　键　词: 间隙泄漏流; 非定常; 近失速工况; 不稳定; 突尖型失速

中图分类号: TK474.8　　文献标识码: A

引　言

现代航空发动机追求更高的总体性能, 更高的单级压比和效率, 在更少的级数上实现更高的负荷成为压气机/风扇追求的目标。然而, 风扇/压气机载荷越高, 对其稳定工作裕度条件的要求也更加苛刻。叶顶间隙泄漏流在压气机内部流动失稳过程中所起的关键作用, 已经成为了共识。

间隙泄漏流不仅严重影响压气机性能, 而且也影响压气机的稳定性, 因此受到国内外研究者的普遍关注。Schlechtriem 和 Hofmann 认为, 顶部间隙泄漏涡破裂(由于激波与间隙泄漏涡相互作用产生的)是导致跨音速压气机转子内部流动失稳的主要因素[1~2]。Hah 对跨音速压气机的研究表明[3], 当相邻叶片压力面前缘附近出现间隙泄漏流溢出时, 该跨音速压气机转子开始失速。Yamada 针对相同跨音速压气机转子[4], 进行时间精确数值模拟[5~6], 研究了间隙泄漏流破裂非定常性。Beigner 和 Hah 分别就某跨音速压气机转子内部流动进行实验测量和数值模拟, 研究认为顶部间隙泄漏流的非定常性以及间隙泄漏流和激波的非定常干涉, 是导致该跨音速压气机转子出现突发型旋转失速的主要原因。国内学者聂超群、卢新根对间隙泄漏流影响跨音速压气机稳定性同样做了大量研究[7~9]。

本文针对跨音速压气机 NASA 转子 37, 采用单通道非定常以及多通道非定常数值模拟, 研究近失速工况条件, 不同背压, 间隙泄漏流非定常流动特性及触发旋转失速, 进一步认清该跨音速压气机转子间隙泄漏流非定常特性、触发失速以及对压气机稳定性影响。

1　研究对象

本文研究对象为跨音速压气机转子(NASA 转子 37), NASA 转子 37 是 1978 年由 NASA Lewis 研究中心为研究展弦比和载荷对压气机性能影响而设计的低展弦比跨音速进口级之一, 表 1 列出了该压气机转子的基本几何参数和气动设计参数。本文的计算都是在该压气机转子 100%设计转速下进行的, 此时该压气机转子叶顶间隙为0.365 mm。

表 1　NASA 转子 37 主要结构参数和设计参数

	数　值
设计流量/kg·s^{-1}	20.19
堵塞流量/kg·s^{-1}	20.93±0.14
总压比	2.106
转速/r·min^{-1}	17 188
等熵效率	0.889
叶片数	36
顶部稠度	1.288
进口轮毂比	0.70
展弦比	1.19
叶型	多圆弧叶型
叶顶相对 Ma	1.48

收稿日期: 2007－10－29;　修订日期: 2007－11－05
基金项目: 航空科学基金资助项目(05C53016).
作者简介: 张燕峰(1983－), 男, 上海人, 西北工业大学博士研究生.

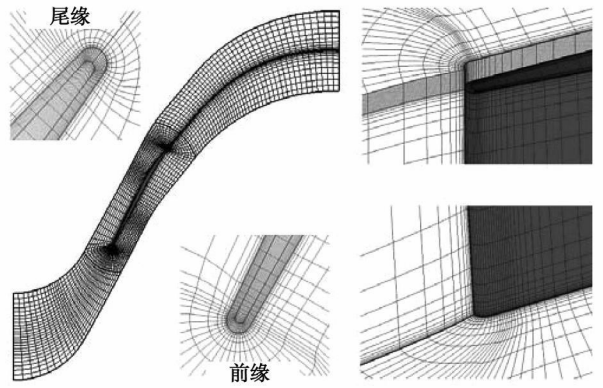

图 1 计算网格示意图

2 数值计算方法

数值计算利用西北工业大学动力与能源学院并行平台 NUMECA /FINE 的 Euranus 求解器, 该平台共 13 个节点, 26 个 CPU, 26 GB 内存。计算过程中采用 Jameson 的有限体积差分格式, 并结合 Spalart－Allmaras 湍流模型对相对坐标系下的三维雷诺平均 Navier－Stokes 方程进行求解, 采用显式四阶 Runge－Kutta 法时间推进以获得定常解。非定常计算采用了隐式双时间方法, 计算中以近失速工况条件下的定常计算结果为非定常计算初场, 且每一个物理时间步长为 1e－5, 每一物理时间步下的虚拟时间步为 20。

为了获得较好的网格正交性, 转子叶片通道采用了 H－O－H 型结构化网格, 叶顶间隙区采用蝶形网格拓扑结构(O 型网格内嵌有 H 型网格), 网格拓扑如图 1 所示; 定常计算时, 卢新根通过网格依赖试验发现主通道采用周向 33 个网格[9], 轴向 249 个网格, 径向 77 个网格, 网格总数约 77 万的网格已经达到了网格无依赖性要求; 非定常计算时, 为了能更详细地捕捉流场细节, 本文通过对计算网格进行加密, 加密后的总共网格数约为 184 万。为了捕捉旋转失速沿叶片周向的非均匀流场, 采用了多通道非定常计算。由于受计算资源限制, 且突尖型旋转失速一般占 2～3 个叶片通道[10], 本文用 6 通道进行非定常计算, 其网格为单通道加密后计算网格沿周向复制, 6 通道网格总数约为1 100万。

3 结果及分析

由于本研究主要关心近失速工况间隙泄漏流的非定常流动, 不讨论定常计算结果。单通道非定常、多通道非定常计算是在两个不同出口背压下进行的, 且两者背压相差1 000 Pa(近失速工况 1< 近失速工况 2)。图 2 为单通道非定常、多通道非定常计算进口流量监测图, 从图 2(a)中可以看出, 单通道计算时, 两种背压下非定常扰动周期明显, 约为 150 个迭代时间步。背压 1 条件下进口流量基本保持不变, 可见在该情况下非定常流动是稳定的, 文献[11]研究发现该非定常流动主要表现为间隙泄漏流的非定常性。而背压 2 条件下流量逐渐减小, 可见非定常流动是不稳定的, 但是计算没有发散(数值失速), 非定常周期未变化; 而图 2(b)中虽然计算初始条件相同, 但是在背压 2 条件下多通道计算表明, 叶片通道已经进入数值失速, 周期性不存在, 这是由于单通道非定常计算初始时刻流场偏离背压 2 条件下的流场结构, 随着计算的进行, 逐渐接近真实流场(背压 2 条件), 在此背压下, 流场逐渐不稳定, 流量在减小,

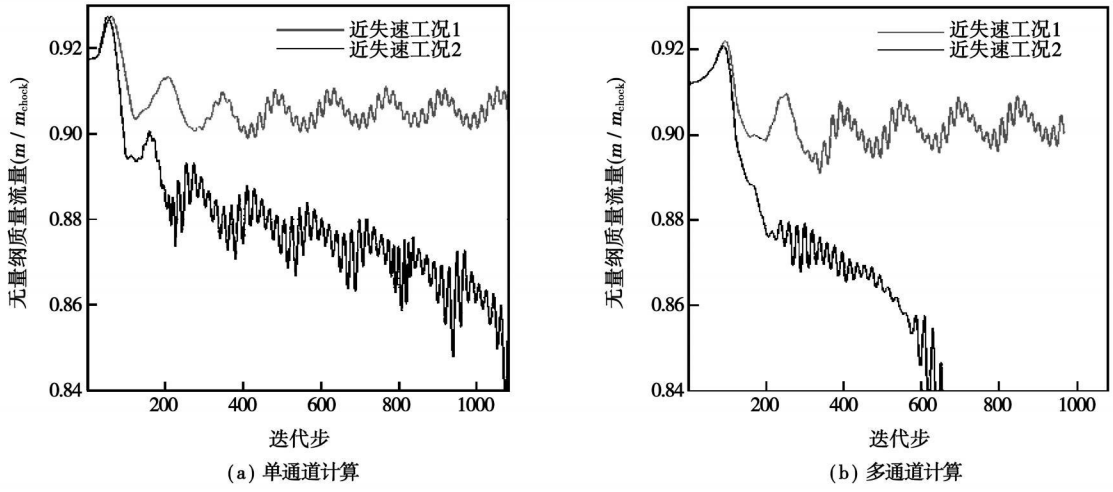

图 2 进口流量监测图

流场渐渐进入数值失速。单通道非定常计算只能模拟失速前流场的结构及失速后流场定性结构, 而多通道非定常计算弥补了单通道模拟的缺陷, 可以准确地模拟触发失速起始时刻的周向非均匀流场及失速后的流场特性; 背压 1 条件间隙泄漏流非定常性稳定, 间隙泄漏流非定常周期性依旧存在, 约为 150 个迭代时间步。

为了能更清楚地认清近失速工况不同背压下, 间隙泄漏流非定常的稳定性, 如图 3 所示 $t=3/8\,T$ 时刻叶顶绝对涡量分布及粒子示踪图, 从图中可以看出, 在相同时刻下, 背压 2 条件下叶顶区域流场扰动强度大, 泄漏流强度明显比背压 1 条件强, 且间隙泄漏流能够碰撞到相邻叶片压力面, 而背压 1 条件下的泄漏流强度弱, 泄漏流没有碰撞到相邻叶片压力面。图 4 为 $t=3/8\,T$ 和 $7/8\,T$ 时刻叶片吸力面极限流线及标准螺旋度图, 其中标准螺旋度 Hn 定义为:

$$Hn=\frac{\vec{\xi}_{\vec{w}}}{|\vec{\xi}||\vec{w}|}$$

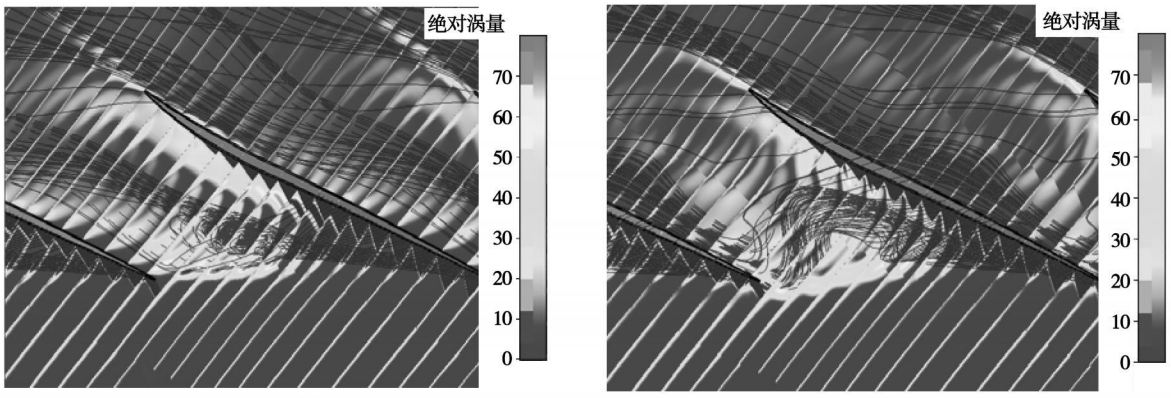

(a) 背压 1 条件　　(b) 背压 2 条件

图 3　$t=3/8\,T$ 时刻叶顶绝对涡量分布及粒子示踪图

式中: $\vec{\xi}$、$\vec{w}$—绝对涡矢量和相对速度矢量; 标准螺旋度 Hn 物理意义为: 计算绝对涡矢量和相对速度矢量的余弦。由图中可以看出, 吸力面极限流线及标准螺旋度大小的变化主要集中在距叶顶 20%处, 即为泄漏流影响区域, 吸力面均出现了分离线和再附线。在背压 1 条件下, 两个时刻的极限流线及标准螺旋度基本没有变化, 主要是由于前面提到的泄漏流强度不够强, 不足以影响叶片吸力面流动; 而在背压 2 条件下, 吸力面上半部分极限流线及标准螺旋度变化明显, 尤其是在叶顶处, $t=3/8\,T$ 时刻, 吸力面分别产生了一个鞍(Saddle)、焦点(Focus)以及节点(Node), 而在 $t=7/8\,T$ 时刻又产生一个焦点, 在此时刻, 吸力面有一个鞍、节点以及两个焦点, 它们在吸力面上的位置也发生了明显的变化。

虽然在背压 2 条件下, 吸力面极限流线及标准螺旋度变化明显, 但是前面提到, 相同条件下多通道非定常计算显示: 该背压下, 间隙泄漏流非定常是不稳定的, 泄漏流前缘溢流诱发压气机转子进入失速。如图 5 所示, 为背压 2 条件下 $t=0$ 时刻, 99%叶高相对速度矢量分布图, 由图中可以看出, 由于泄漏流非定常的不稳定, 使得叶片某一通道突然出现泄漏流在叶片前缘溢出, 从而诱发该压气机转子失速先兆。对于单通道非定常计算, 捕捉不到这种周向扰动, 从而单通道非定常计算虽然观测到间隙泄漏流非定常的不稳定, 但是不能进一步分析这种不稳定对流场结构的影响。图 6 为背压 2 条件下 $t=1.375$ 时刻, 99%叶高相对马赫数分布图, 可以看出此时叶片通道已经进入数值失速。

4　结　论

针对 NASA 转子 37 跨音速压气机做了单通道非定常及多通道非定常数值模拟, 得到如下结论:

(1) 在近失速工况下, 单通道非定常计算结果揭示了该压气机转子存在间隙泄漏流自身非定常性, 然而不同背压条件下, 会影响间隙泄漏流非定常性的稳定。较大背压(背压 2)情况下, 间隙泄漏流非定常性很不稳定, 具体体现在流量的逐渐减小, 但是泄漏流非定常周期性依然存在; 较小背压(背压 1)情况下, 间隙泄漏流非定常性稳定。

(2) 近失速工况下, 不同背压计算泄漏流的非定常周期相同, 约为 150 迭代时间步, 但是对间隙泄

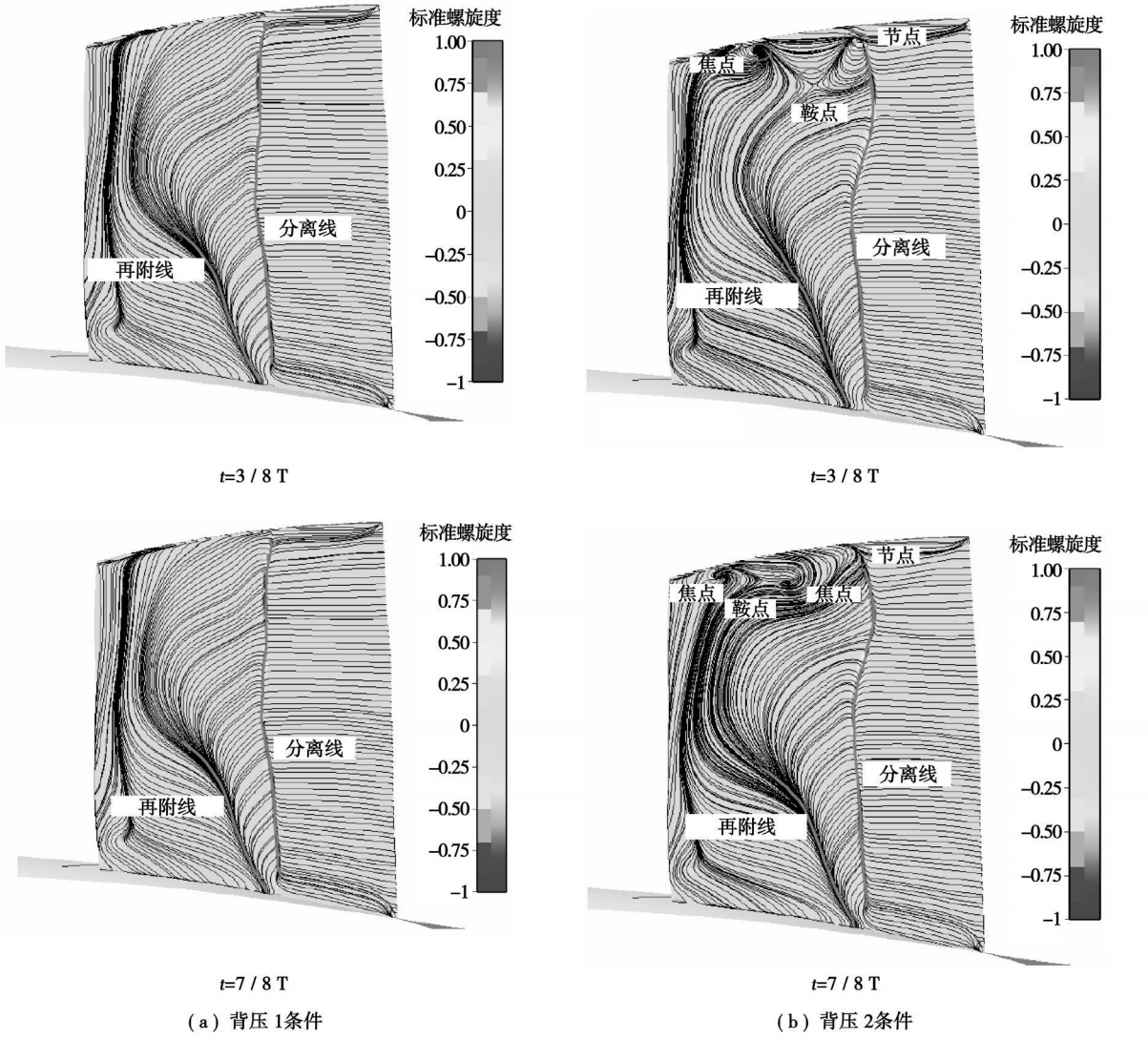

图 4 $t=3/8T$ 和 $7/8T$ 时刻吸力面极限流现及标准螺旋度

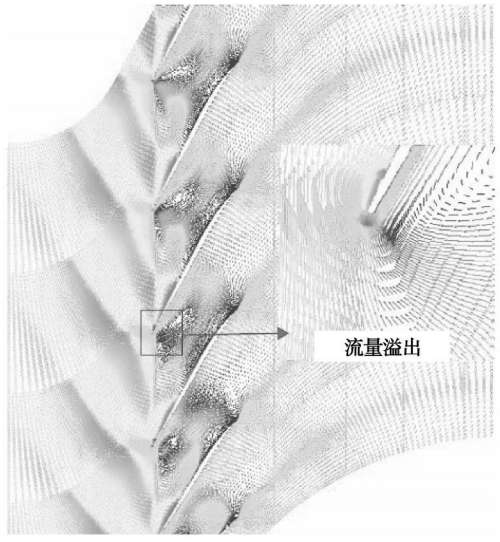

图 5 $t=0$ 时刻 99%叶高相对速度矢量图

图 6 $t=1.375$ 时刻 60%轴向弦长截面相对 *Ma* 分布

漏流强度影响较大。较大背压(背压 2)情况下, 泄漏流强度较大, 泄漏流可以和相邻叶片压力面碰撞, 叶片吸力面上半部分存在鞍点、焦点和节点, 其位置及数目随时间发生变化。较小背压(背压 1)情况下, 泄漏流强度弱, 不能与相邻叶片压力面碰撞, 且吸力面流动结构基本没有变化。

(3) 多通道非定常数值模拟揭示: 在背压 2 条件下, 间隙泄漏流非定常随机振荡诱发该跨音速压气机转子突尖型旋转失速先兆, 失速团首先在叶尖形成, 最终进入数值失速, 泄漏流的周期性遭到破坏; 在背压 1 条件下, 泄漏流非定常性稳定, 其周期性始终存在。

参考文献:

[1] SCHLECHTRIEM S, LOTZERICH M. Breakdown of tip leakage vortices in compressors at flow conditions close to stall[R]. ASME Paper 97-GT-41, 1997.

[2] HOFFMAN W H, BALLMAN J. Some aspects of tip vortex behavior in a transonic turbocompressor[R]. ISABE Paper 2003-1223, 2003.

[3] HAH C, RABE D C. Role of tip clearance flows on flow instability in axial flow compressors[R]. ISABE, 2001-1223, 2001.

[4] YAMADA K, FURUKAWA M, INOUE M, et al. Unsteady three-dimensional flow phenomena due to breakdown of tip leakage vortex in a transonic axial compressor rotor[R]. ASME Paper: GT2004-53745, 2004.

[5] HAH C, BERGNER J, SCHIFFER H. Short length-scale rotating stall inception in a transonic axial compressor-criteria and mechanisms[R]. ASME Paper: 2006-GT-90045, 2006.

[6] BERGNER J, KINZEL M, SCHIFFER H, et al. Short length-scale rotating stall inception in a transonic axial compressor-experimental investigation[R]. ASME Paper: 2006-GT-90209, 2006.

[7] 聂超群, 桂幸民, 于　清, 等. 跨音压气机近失速状态的非定常特征[J]. 工程热物理学报, 1999, 20(2): 171-175.

[8] 卢新根, 楚武利, 张燕峰. 跨音速压气机顶部间隙泄漏流与处理机匣之间相互作用分析[J]. 西安交通大学学报, 2006, 40(11): 1359-1360.

[9] 卢新根. 轴流压气机内部流动失稳及其被动控制策略研究[D]. 西安: 西北工业大学博士论文, 2007.

[10] VO H D, TAN C S, GREIZER E M. Criteria for spike initiated rotating stall[R]. ASME Paper: 2005-GT-68374, 2005.

[11] 张燕峰, 楚武利, 吴艳辉, 等. 跨音速轴流压气机近失速状态间隙泄漏流非定常流动研究[R]. 中国工程热物理学会热机气动热力学会议, 2007.

(编辑　刘　伟)

新技术、新工艺

CLN 蒸汽回注限制 NO_x 排放低于 5 mg/kg

据《Gas Turbine World》2008 年 3~4 月号报道, IPT(国际动力技术公司)已利用 CLN(程氏低 NO_x)喷嘴蒸汽回注以保守的蒸汽与燃料比, 在增加装置效率和输出功率的同时在 Allison 501-KB5 燃气轮机上达到了超低排放级。

排放: 针对商业的改型性能, IPT 保证在 1 035 ℃涡轮入口燃烧温度下达到 5 mg/kg NO_x 和 80 mg/kg CO 或更少的排放。

预算价格: 整套承包价格在 235 000~295 000 美元范围内, 不包括燃烧火焰筒和发动机外的蒸汽源。

低 NO_x 喷嘴: 设计特色是大直径的燃料——蒸汽进口孔(以便使背压减到最小)和可拆的顶部(以便降低喷嘴维护费用)。喷嘴直径、孔和流动角是专门设计, 以便匹配燃烧火焰筒。

发动机外混合: 利用程氏低 NO_x 回注, 蒸汽和燃料可以在发动机外混合, 达到高度的均匀性。并且燃料气体可在混合前加热, 以防止任何冷凝的可能性。这些设计变化能达到更低的 NO_x 排放。

(吉桂明　供稿)

lytical results can provide some guidance for evaluating the operation of the unit. **Key words**: elevation, rotor, transfer matrix, turbo－generator unit

三维全息谱在诊断负荷诱发的转子热弯曲与标高故障中的运用＝**Application of Three－dimensional Holographic Spectrums in the Diagnosis of a Load－induced Rotor Thermal Bending and Elevation Fault**[刊, 汉] / WANG Xiu－feng, QU Liang－sheng, LIAO Yu－he (Intelligent Instrument and Monitoring/Diagnosis Research Institute, Xi' an Jiaotong University, Xi' an, China, Post Code: 710049)// Journal of Engineering for Thermal Energy & Power. － 2008, 23(5). －462 ~467

It is extremely common for a large－sized rotary machine to undergo a vibration change of its shafting resulting from a load variation during its operation. An abnormal vibration is often triggered by a change of such operating conditions as the transfer torque and thermal state, etc. of a bearing－rotor system experiencing load variations. The authors have combined the load－induced vibration mechanism with three－dimensional holographic spectrum technology and fully utilized the shafting vibration information indicated by a three－dimensional holographic spectrum to identify the three－dimensional holographic spectrum characteristics of different faults, thus providing a new approach for discriminating load－induced vibration faults. The mechanism and three－dimensional holographic spectrum characteristics of a thermal bending and elevation fault have been analyzed. The verification results obtained from on－site data show that the spectrum characteristics in question resulting from a mechanism analysis enjoy a good ability to identify load－induced vibration faults. **Key words**: holographic spectrum, vibration, thermal bending, elevation, load

冲角对高负荷正弯叶栅壁面静压影响的实验研究＝**Experimental Study of the Effect of an Incidence on the Wall－surface Static Pressure of a High－load Positively－bent Cascade**[刊, 汉] / CHEN Shao－wen, LIU Shun－long (College of Power and Energy Source Engineering, Harbin Engineering University, Harbin, China, Post Code: 150001), BIAN Zhao－xi (Harbin Ha－dian Electrical Co. Ltd., Harbin, China, Post Code: 150001)// Journal of Engineering for Thermal Energy &Power. － 2008, 23(5). －468 ~472

An experimental study has been conducted of the effect of an incidence on the wall surface static pressure of a high－load annular positively－bent diffusion cascade. The results of the study show that when the incidence is positive, the suction surface of a straight－blade cascade exhibits an evident tendency of reverse "C" shaped pressure distribution, which will be intensified with an increase of the bending angle and result in a gradual accumulation of low－energy fluid in the middle of the blade span. Due to a relatively strong reverse pressure gradient streamwise on the suction surface, the air flow in the middle blade span is prone to be separated, thus causing a sharp increase of losses. In a high－load compressor cascade, when the incidence is negative and zero, the adoption of a positively－bent blade design will lead to a better effectiveness in reducing separation and losses than in the case when the incidence is positive. In addition, an excessively large bending angle should be avoided. **Key words**: experimental study, high－load cascade, positive bending, incidence, static pressure

跨音速轴流压气机间隙泄漏流流动特性研究＝**A Study of the Clearance Leakage Flow Characteristics of a Transonic Axial－flow Compressor**[刊, 汉] / ZHANG Yan－feng, CHU Wu－li, WU Yan－hui (College of Power and Energy Source, Northwestern Polytechnical University, Xi' an, China, Post Code: 710072)// Journal of Engineering for Thermal Energy &Power. － 2008, 23(5). －473 ~477

Clearance leakage flow exercises a major influence on the formation of rotating stall of an axial flow compressor. The authors have conducted a single－passage and multi－passage non－steady numerical simulation by utilizing the transonic axial－flow compressor of NASA rotor 37. The single－passage non－steady calculation results reveal that at an operating condition approximating to compressor stalling speed, there exists a clearance leakage－flow self non－steady behavior at the blade tip. In addition, the non－steady simulation results under two different back－pressure conditions have been compared. When the back pressure at the outlet is comparatively high, the unsteady behavior of the clearance leakage flow is extremely unstable. When the back pressure at the outlet is relatively low, the above－mentioned unsteady behavior is stable. The multi－passage non－steady numerical simulation results indicate that at an operating condition approximating to the stalling speed, when the outlet back pressure is comparatively high, the clearance leakage flow will oscil-

late unsteadily, triggering the inception of a spike type rotating stall and resulting in a concrete embodiment of overflow from the blade tip leakage at the leading edge. However, when the outlet back pressure is relatively low, the unsteady behavior of the clearance leakage flow has all along been relatively stable. **Key words**: clearance leakage flow, non—steady, near—stall operating condition, unstable

某电站燃气轮机温控系统故障分析=**Fault Analysis of the Gas Turbine Temperature Control System of a Power Plant**[刊, 汉] / JIN Wei—wu (Wuxi Subsidiary, Harbin No. 703 Research Institute, Wuxi, China, Post Code: 214151), CHEN Cai—wang, HE Dong—lin, TIAN Ming—quan (Tarim Oil Field Sub—company, Southwest Tarim Power Company, Ze—pu Petroleum Base, China, Post Code: 844804)// Journal of Engineering for Thermal Energy & Power. — 2008, 23(5). —478 ~480

The authors have studied the fault phenomenon that has often befallen the gas turbine temperature control system of a power plant and performed a detailed analysis of the phenomenon in conjunction with a model for the above control systems. Through a comparison of the influence of various correction parameters of the above—cited model on control effectiveness, presented were the countermeasures for dealing with the faults of the control system in question. The tests under various operating conditions show that the countermeasures proposed can effectively eliminate the faults of the temperature control system, providing valuable experience for the commissioning tests and operation of gas turbine power plants of a similar type. **Key words**: gas turbine, temperature control system, fault

有隔热涂层的气膜冷却火焰筒壁温计算=**Wall Temperature Calculation of an Air—film Cooled Flame Tube with a Heat Insulation Coating**[刊, 汉] / LI Ming—jia, LIN Feng, LI Wei—shun (Harbin No. 703 Research Institute, Harbin, China, Post Code: 150036), QU Zhe (Harbin Power Plant Engineering Co. Ltd., Harbin, China, Post Code: 150040)// Journal of Engineering for Thermal Energy & Power. — 2008, 23(5). —481 ~484, 515

With a thin—wall flame tube serving as an object of study, presented was a wall temperature calculation model and method for an air—film cooled flame tube with a heat insulation coating. By using the method in question, the wall temperature of the flame tube of an annular—tube combustor was calculated with the possible cause of a crack occurring to the primary main combustion hole of the flame tube being identified. In addition, the influence of the air—film cooling, heat insulation coating and its thickness on the radial and axial distribution of the flame tube wall temperature was also studied. The results of the study show that the maximum wall temperature of the flame tube at 946 ℃ can meet the design requirement for the maximum wall temperature of the flame tube. The wall surface temperature distribution gradient near the primary main combustion hole on the flame tube is relatively big, where a thermal stress concentration is liable to be located, providing an underlying basis for identifying the cause of any fault occurring to the flame tube. The air—film cooling and heat insulation coating can remarkably lower the wall temperature of the flame tube and effectively improve the wall temperature radial and axial distribution on the latter. The heat insulation coating thickness exercises a very small influence on the wall temperature of the flame tube. **Key words**: flame tube, heat insulation coating, air—film cooling, wall temperature calculation

并联型化工动力多联产系统主导因素与变工况特性=**Leading Factors and Off—design Operating Condition Characteristics of the Power Polygeneration System of a Parallel—type Chemical Engineering Unit**[刊, 汉] / FENG Jing, NI Wei—dou, LI Zheng (Thermal Energy Engineering Department, Tsinghua University, Beijing, China, Post Code: 100084)// Journal of Engineering for Thermal Energy & Power. — 2008, 23(5). —485 ~489

Electric power is one of the main products of a polygeneration system. Therefore, it will unavoidably encounter load variation problems during its operation. From a load variation viewpoint, the authors have mulled how to design a polygeneration system to meet the requirements of an electric network. Through a detailed simulation analysis, two leading factors influencing the load variation ability of the parallel polygeneration system have stood out, i.e. design power/chemical ratio and synthetic unit capacity surplus. The relationship of the leading factors and the system load variation ability was shown in the form of a four—quadrant chart. In addition, the characteristics of the system operating during load variations were further analyzed. The results of the analysis reveal the law governing the load distribution between a power generation unit and chemical engineering one during the load variation operation of the polygeneration system as well as the